Supplementary Data for

A Receptor-like Protein Acts as a Specificity Switch for Regulation of Stomatal Development

Guangzhong Lin[1,2], Liang Zhang[3], Zhifu Han[1], Xinru Yang[1], Weijia Liu[1], Ertong Li[4], Junbiao Chang[5], Yijun Qi[6], Elena D Shpak[3] and Jijie Chai[1,6,7,8]*

[1]Innovation Center for Structural Biology, Tsinghua-Peking Joint Center for Life Sciences, School of Life Sciences, Tsinghua University, Beijing 100084, China.

[2] College of Life Sciences, Peking University, Beijing 100871, China.

[3]Biochemistry, Cellular & Molecular Biology, University of Tennessee, M407 Walters Life Science, Knoxville, TN 37996, USA.

[4]College of Chemistry and Molecular Engineering, Zhengzhou University, Zhengzhou, 450001, China.

[5]Collaborative Innovation Center of New Drug Research and Safety Evaluation, Zhengzhou University, Zhengzhou, China.

[6]Center for Plant Biology, School of Life Sciences, Tsinghua University, Beijing 100084, China.

[7]Max-Planck Institute for Plant Breeding Research, Cologne, Germany.

[8]Institute of Biochemistry, University of Cologne, Zuelpicher Str. 47, 50674 Koeln, Germany.

*To whom correspondence should be addressed：chaijj@tsinghua.edu.cn

Supplemental Figure S1

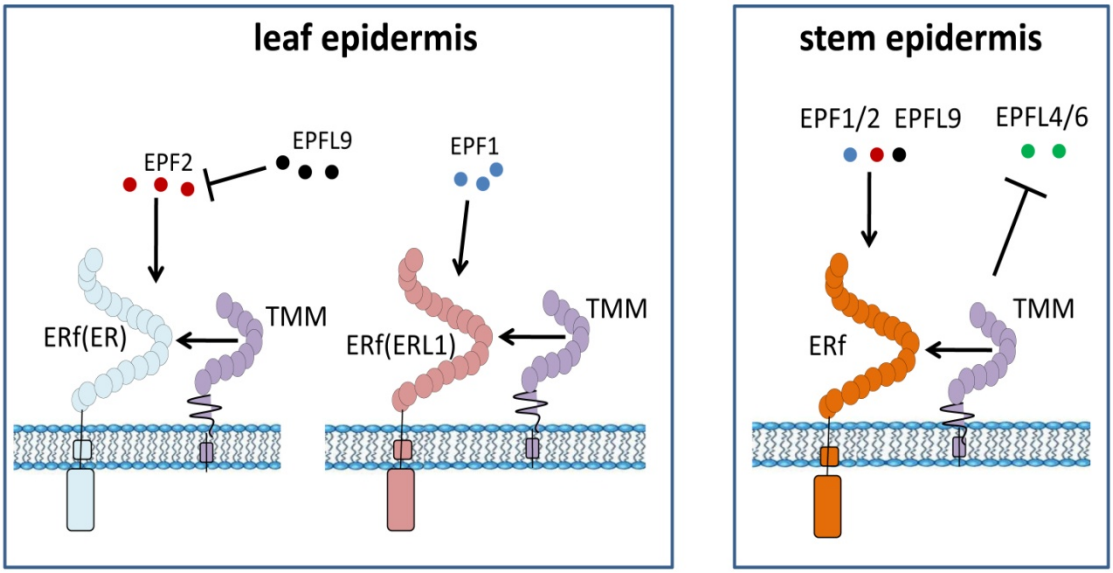

Supplemental Figure S1. Cartoon depicting the roles of EPF peptides, ERf and TMM in stomatal patterning.

In the epidermis of leaves, the secreted peptide EPF2 (red) is produced by meristemoid mother cells (MMCs) and early meristemoids. EPF2 is primarily perceived by ERECTA (light blue) in complex with TMM (purple) and acts to restrict initiation of stomatal cell lineages. EPFL9 (black) is secreted from mesophyll cells and binds to ERf in competition with EPF2, blocking EPF2 signaling. EPF1 (blue), which is secreted by late meristemoids and guard mother cells (GMCs), mainly interacts with ERL1 (pink) in complex with TMM to repress meristemoid differentiation into GMCs and to promote correct spacing of newly formed secondary meristemoids. However, in the epidermis of stems, ERf receptors (orange) if not in complex with TMM can be subject to inappropriate activation by the EPFL4/6 peptides (green), which are normally produced in inner tissues for inflorescence development. TMM functions to repress EPFL4/6-mediated signaling.

Supplemental Figure S2

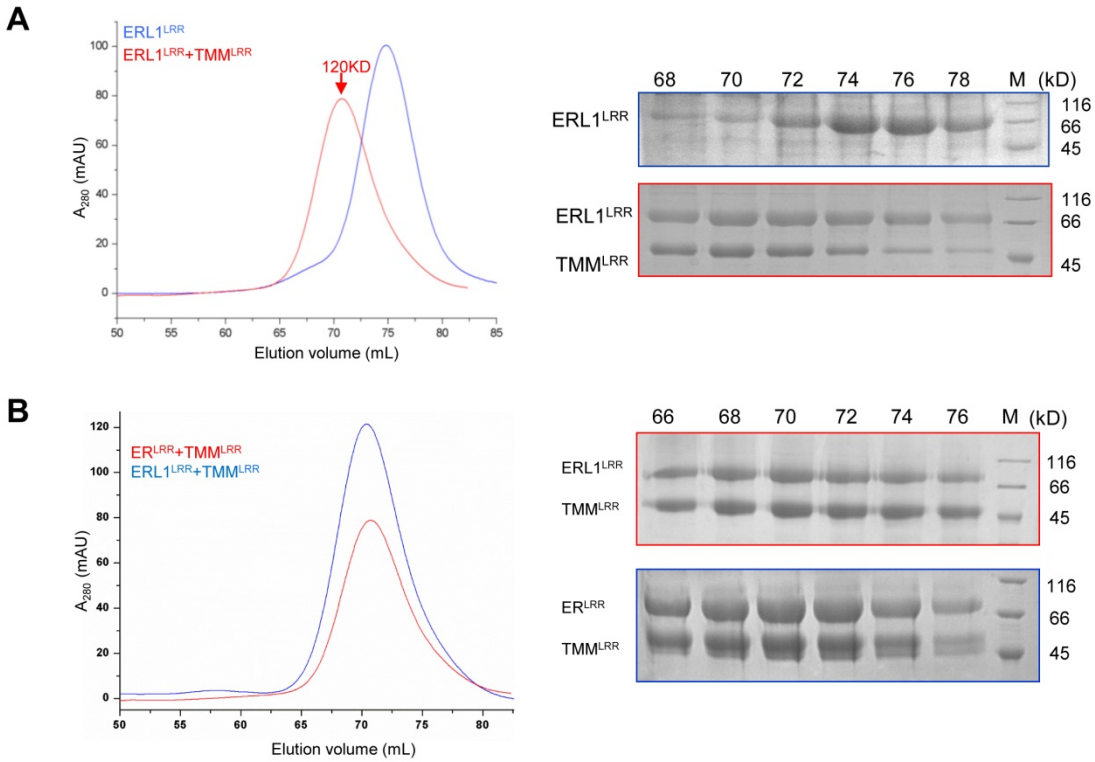

Supplemental Figure S2. ER^{LRR} and ERL1^{LRR} forms complex with TMM^{LRR} *in vitro*.

(A) TMM^{LRR} directly interacts with ERL1^{LRR} *in vitro*. Left, superposition of the gel filtration chromatograms of the ERL1^{LRR} and ERL1^{LRR}-TMM^{LRR} proteins. The vertical and horizontal axes represent UV absorbance (280 nm) and elution volume (ml), respectively. Bottom, Coomassie blue staining of the peak fractions shown on the top following SDS-PAGE. "M": molecular weight ladder (kD).

(B) Size-exclusion chromatography analysis (left panel) of the interaction between ER^{LRR} or ERL1^{LRR} and TMM^{LRR}; SDS–PAGE analysis (right panel) of peak fractions from the left panel.

Supplemental Figure S3

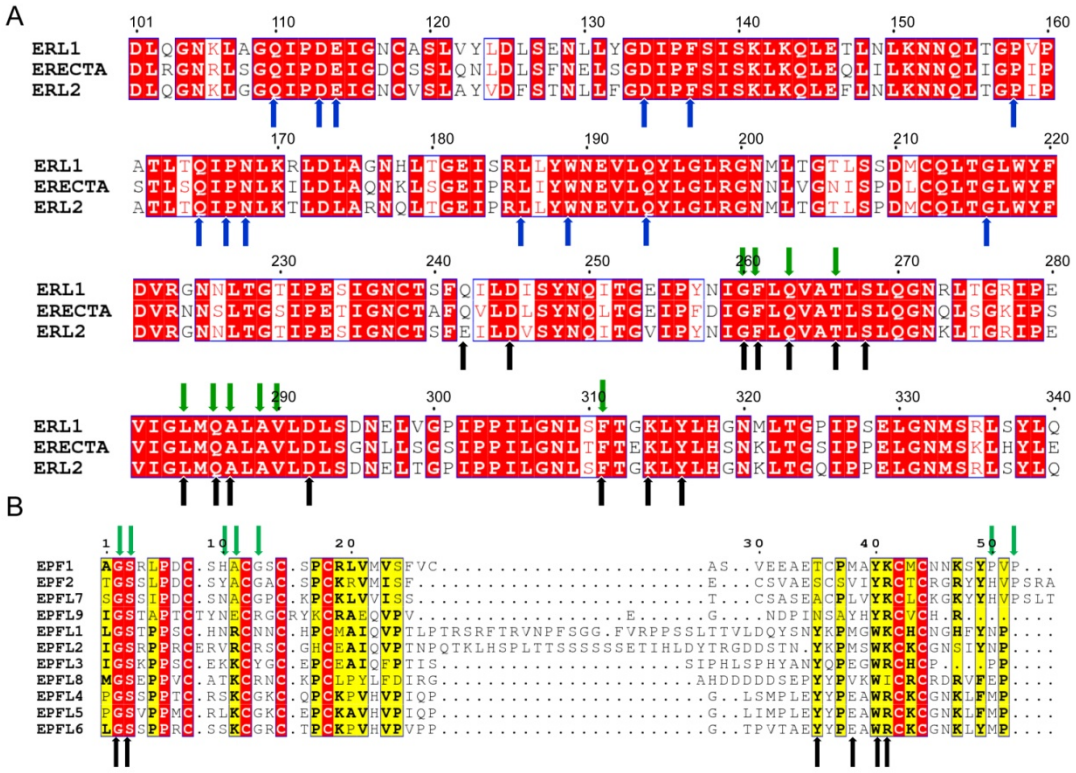

Supplemental Figure S3. TMM^{LRR}- and EPFs-interacting residues are conserved among ERfs and EPFs, respectively.

(A) Sequence alignment of the ectodomains of ERfs. Conserved and similar residues are boxed with red ground and red font, respectively. Residues involved in interaction with TMM and recognition of EPF1/2 are indicated with blue and green arrows at the bottom and top, respectively. Residues involved in EPFL4 binding are indicated with black arrow at the bottom.

(B) Sequence alignment of EPFL peptides. Conserved and similar residues are boxed with red and yellow ground. Residues of EPF1 interacting with ERL1^{LRR}-TMM^{LRR} are indicated with green arrows on the top and residues of EPFL4 interacting with ERL2^{LRR} are indicated with black arrows at the bottom.

Supplemental Figure S4

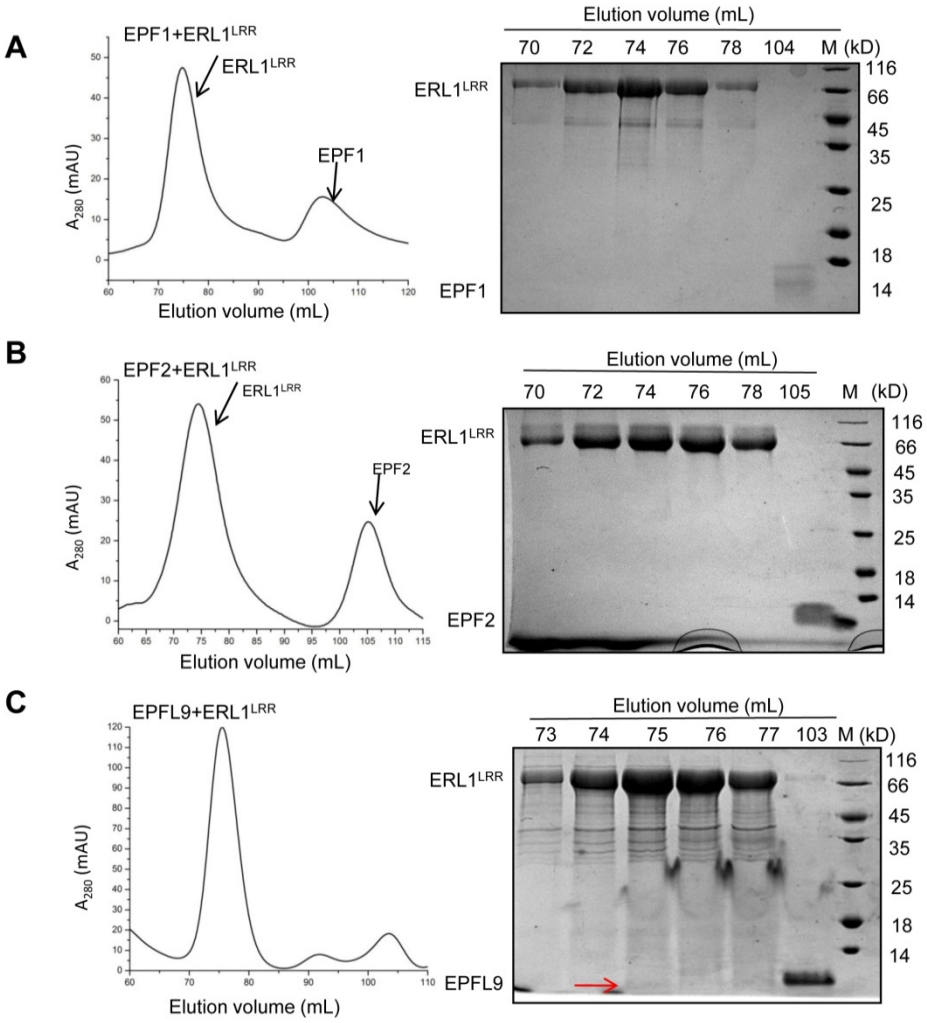

Supplemental Figure S4. EPF1 or EPF2 fail to interact with ERL1^{LRR} alone, whereas EPFL9 shows weak activity of interacting with ERL1^{LRR} in gel filtration.

(A) Size-exclusion chromatography analysis (left panel) of the interaction between ERL1^{LRR} and EPF1; SDS–PAGE analysis (right panel) of peak fractions from the left panel.

(B) Size-exclusion chromatography analysis (left panel) of the interaction between ERL1^{LRR} and EPF2; SDS–PAGE analysis (right panel) of peak fractions from the left panel.

(C) Size-exclusion chromatography analysis (left panel) of the interaction between ERL1^{LRR} and EPFL9; SDS–PAGE analysis (right panel) of peak fractions from the left panel. The band of EPFL9 is indicated by red arrow.

Supplemental Figure S5

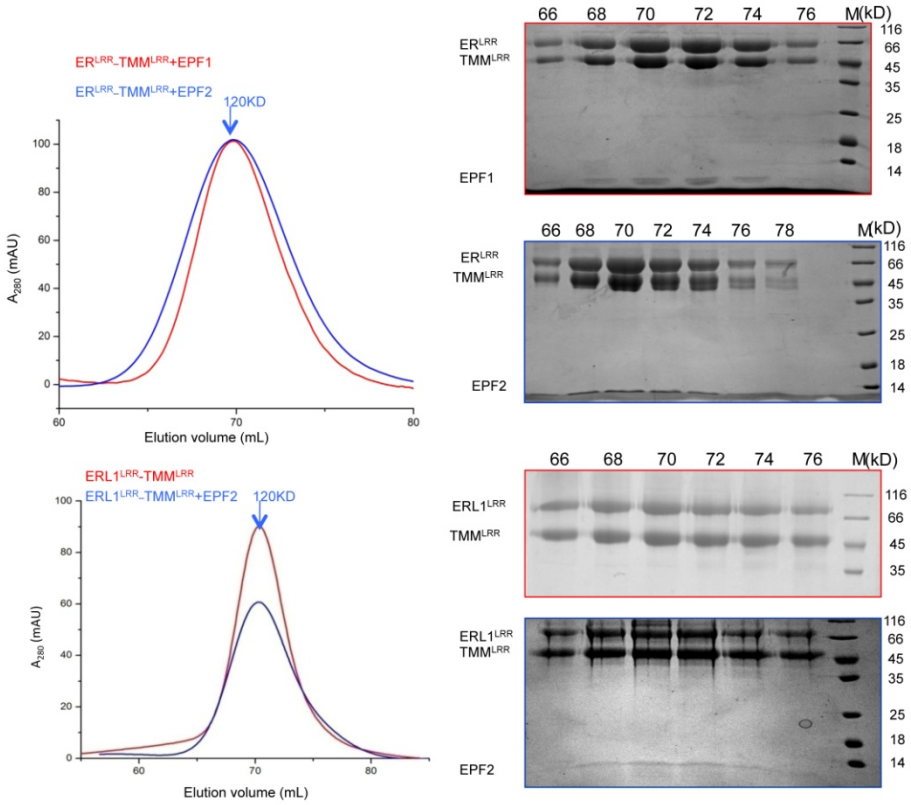

Supplemental Figure S5. EPF1/2 interaction with ER^{LRR}-TMM^{LRR} or ERL1^{LRR}-TMM^{LRR} in gel filtration.

Size-exclusion chromatography analysis (left panel) of the interaction between ER^{LRR}-TMM^{LRR} or ERL1^{LRR}-TMM^{LRR} and EPF1 or EPF2; SDS–PAGE analysis (right panel) of peak fractions from the left panel.

Supplemental Figure S6

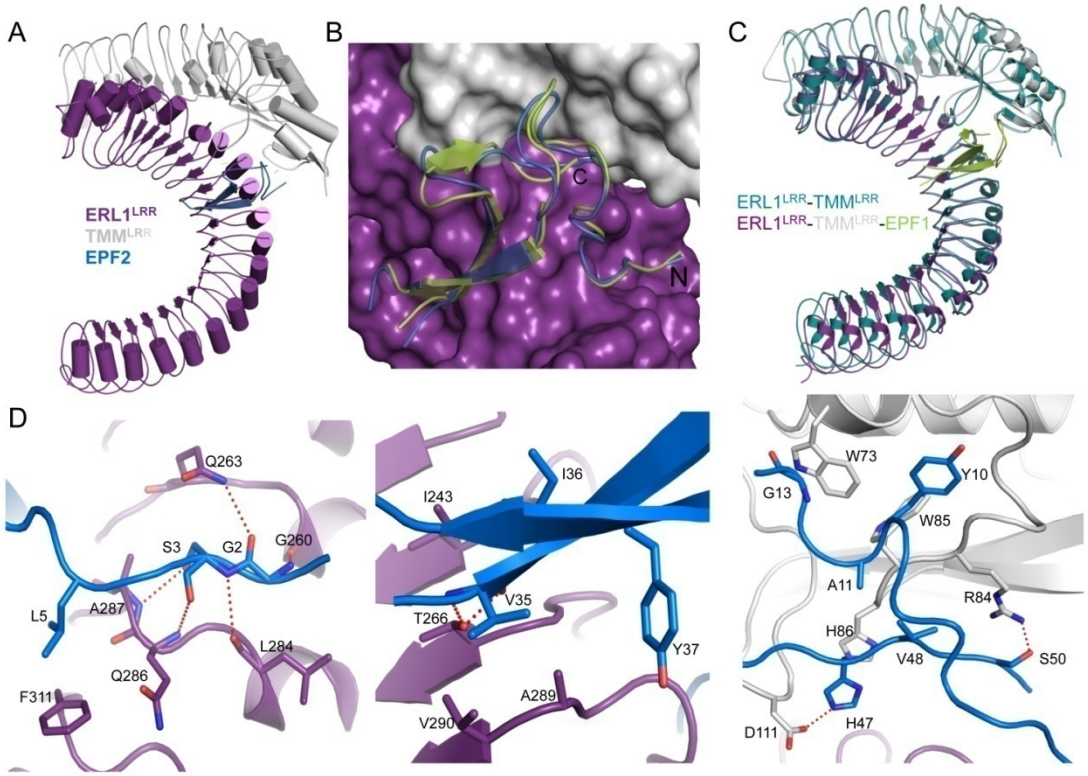

Supplemental Figure S6. Recognition mechanism of EPF2 by ERL1^{LRR}-TMM^{LRR}.

(A) Overall structure of the EPF2-ERL1^{LRR}-TMM^{LRR} complex. "N" and "C" represent the N and C terminus respectively.

(B) A close-up view of the interaction between EPF1/2 and ERL1^{LRR}-TMM^{LRR}. "N" and "C" represent the N and C terminus respectively.

(C) Structural comparison of ERL1^{LRR}-TMM^{LRR} and ERL1^{LRR}-TMM^{LRR}-EPF1. The structure of ERL1^{LRR} was used as the template for the alignment.

(D) Left: Detailed interactions of the N-terminal side of EPF2 with ERL1^{LRR}-TMM^{LRR}. Middle: detailed interactions of the central region of EPF2 with ERL1^{LRR}-TMM^{LRR}. Right: detailed interactions of EPF2 with ERL1^{LRR}-TMM^{LRR}.

Supplemental Figure S7

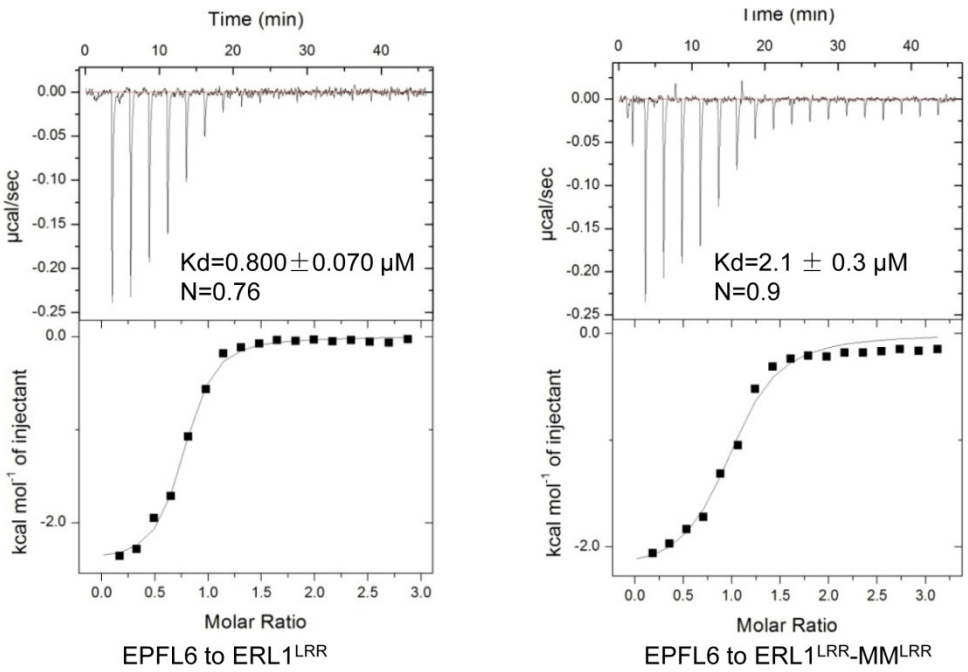

Supplemental Figure S7. TMM dampens EPFL6 binding to ERL1 *in vitro*.

TMM dampens EPFL6 binding to ERL1 *in vitro*. Quantification of the binding affinity of EPFL6 to ERL1^{LRR} or ERL1^{LRR}-TMM^{LRR} by ITC. EPFL6 was titrated into ERL1^{LRR} or ERL1^{LRR}-TMM^{LRR} protein in the ITC cell. Raw data (upper panel) and integrated heat measurements (lower panel) from ITC are shown. The calculated stoichiometry (N), and the dissociation constant (Kd) are indicated.

Supplemental Figure S8

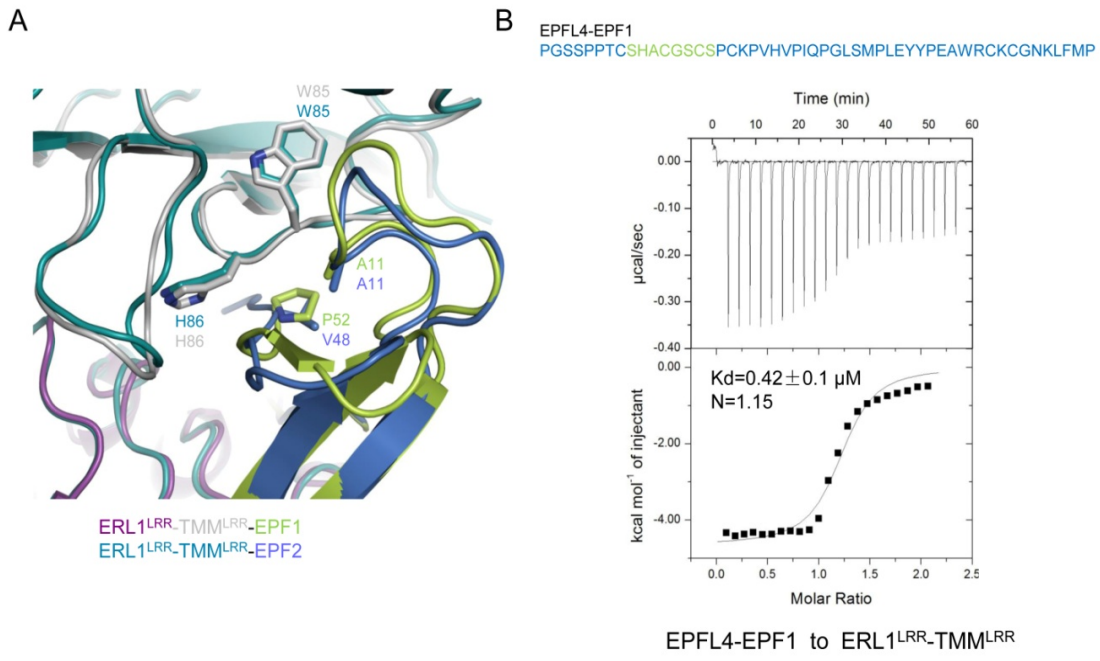

Supplemental Figure S8. The residue A11 of EPF1 and EPF2 is involved in maintaining their structural integrity.

(A) Structural alignment of EPF1-ERL1^{LRR}-TMM^{LRR} and ERL1^{LRR}-TMM^{LRR}-EPF2. Color codes are indicated.

(B) Domain swapping imparts a higher affinity of EPFL4 with ERL1^{LRR}-TMM^{LRR}. Quantification by ITC of the binding affinity of ERL1^{LRR}-TMM^{LRR} with a mutant EPFL4 generated through substituting the apical domain of EPFL4 with that of EPF1. The blue and green letters indicate the amino-acid sequences of EPFL4 and EPF1, respectively. The mutant EPFL4 was titrated into ERL1^{LRR}-TMM^{LRR} complex protein in the ITC cell. Raw data (upper panel) and integrated heat measurements (lower panel) from ITC are shown. The heat of dilution obtained by the titration of peptides into the buffer was subtracted. The calculated stoichiometry (N), and the dissociation constant (Kd) are indicated.

Supplemental Figure S9

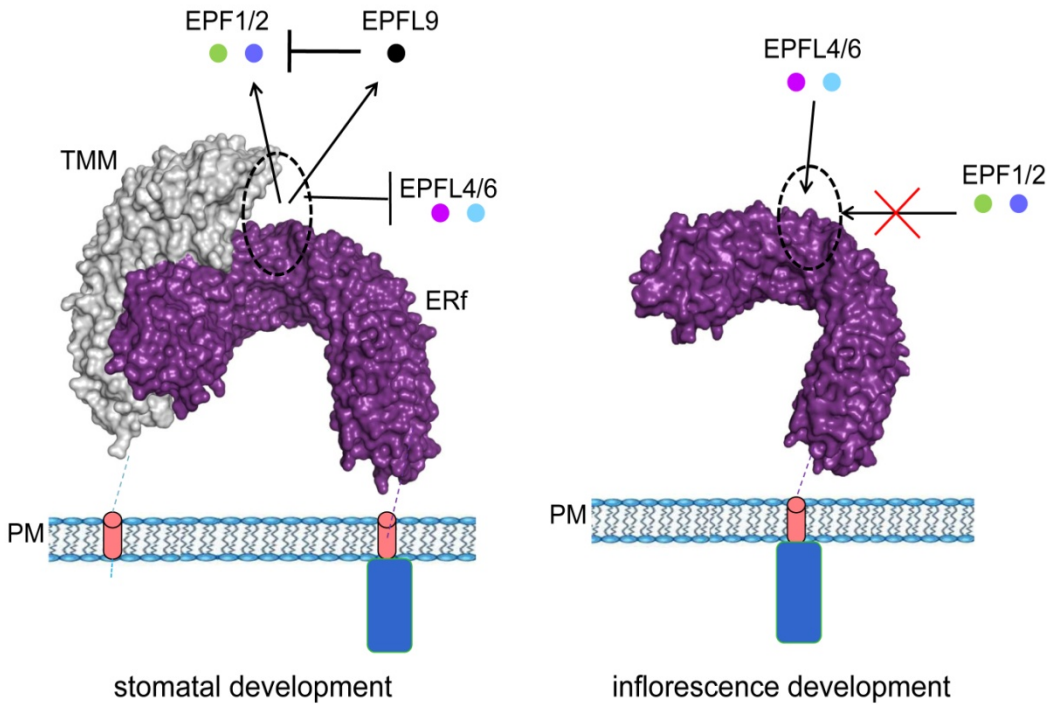

Supplemental Figure S9. A working model of the actions of ERfs and EPFL peptides in stomatal and inflorescence development.

In epidermis (left), TMM and ERf form constitutive complexes to perceive the stomatal regulatory peptides EPF1/2 and EPFL9. These complexes, however, are unfavorable for perception of other peptides such as EPFL4/6. While TMM also promotes perception of EPFL9 by an ERf, the resulting complex is signaling incompetent. EPFL9 competes with EPF1/2 to bind the constitutive complexes, thus dampening EPF1,2-induced signaling. In inflorescence development (right), EPFL4/6 are perceived by the TMM-free ERfs to regulate inflorescence architecture, but EPF1/2 fail to do so due to their inability to bind to the TMM-free ERfs. Dashed ellipses represent the EPF-binding zones.

Supplemental Figure S10

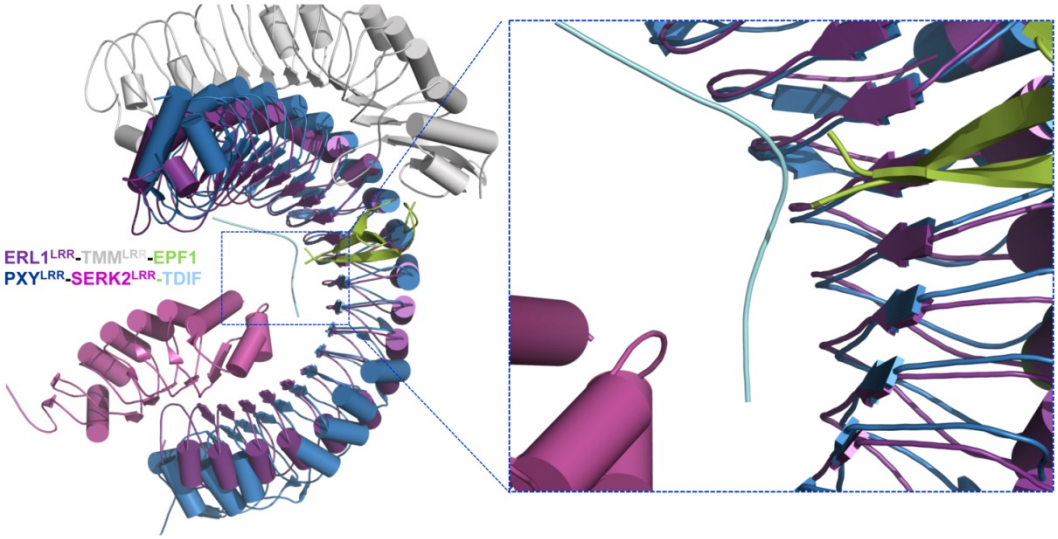

Supplemental Figure S10. Structural alignment of PXY^{LRR}-TDIF-SERK2^{LRR} and EPF1-ERL1^{LRR}- TMM^{LRR}.

Shown on the left is structural alignment of PXY^{LRR}-TDIF-SERK2^{LRR} and ERL1^{LRR}-EPF1-TMM^{LRR} complexes. The structure of PXY^{LRR} was used as the template for the alignment.

Supplemental Figure S11

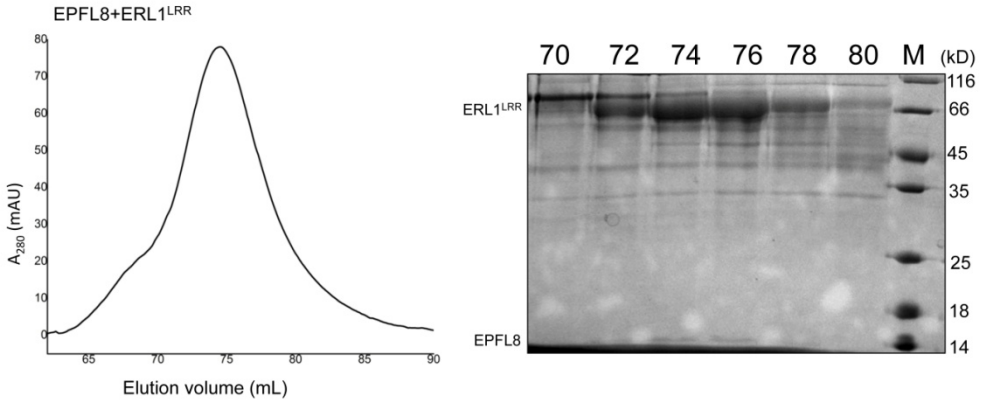

Supplemental Figure S11. EPFL8 directly binds to ERL1^{LRR} independent of TMM^{LRR}.

Size-exclusion chromatography analysis (left panel) of the interaction between ERL1^{LRR} and EPFL8; SDS–PAGE analysis (right panel) of peak fractions from the left panel.

Supplemental Table S1.

Data set	ERL1^{LRR}-TMM^{LRR}	EPF1-ERL1^{LRR}-TMM^{LRR}	EPF2-ERL1^{LRR}-TMM^{LRR}	EPFL4-ERL2^{LRR}
Wavelength (Å)	0.9792	0.9792	0.9792	0.9792
Resolution (Å)	50.0-3.05 (3.10-3.05)	50.0-2.65 (2.70-2.65)	50.0-3.45 (3.51-3.45)	50.0-3.65 (3.71-3.65)
Space group	P1	P1	P1	P212121
a, b, c (Å)	116. 2, 114. 4, 191. 9	66. 1, 66. 1, 143. 5	66. 1, 65. 6, 142. 5	108. 9, 112. 3, 175. 4
α, β , γ (°)	89. 6, 90. 4, 59. 8	97. 6 , 102. 5, 93. 7	97. 6, 102. 8, 93. 6	90.0, 90.0, 90.0
Unique reflections	158,048(14,466)	65,476 (5,984)	29,492 (2,339)	21,816 (1,922)
Completeness	98.5% (98.5%)	94.6% (94.9%)	93.8% (93.0%)	89.6% (89.3%)
Rsym (%)	10.0(49.8)	9.9(39.7)	12.9(50.2)	11.2(54.6)
redundancy	3.0(3.1)	3.2(3.3)	3.0(2.9)	3.5(3.4)
I/δ	14.0(2.8)	16.3(3.4)	6.8(1.7)	13.8(2.9)
Statistics for refinement				
Resolution (Å)	50-3.05 (3.1—3.05)	50.0-2.63(2.66-2.63)	50.0-3.47(3.59-3.47)	50.0-3.65(3.81-3.65)
No. of RFs	157,985(14,466)	65447(5982)	29462(2336)	21781 (1922)
Completeness	97.6%	93.6%	94.6%	88.7%
Rwork/Rfree (%)	18.4 (29.2)/ 24.2(39.3)	23.9(28.3)/ 28.5(38.1)	20.3(20.8)/ 28.2(29.7)	24.2(37.6)/ 30.4(44.3)
R.m.s.d				
Bond (degree)	1.419	1.688	1.936	2.011
length (Å)	0.009	0.011	0.011	0.013
Ramachandran Plot	Favored: 90.6% Allowed: 8.52% Outliers: 0.87%	Favored: 95.6% Allowed: 3.97% Outliers: 0.42%	Favored: 89.1% Allowed: 9.8% Outliers: 1.07%	Favored: 93.2% Allowed: 5.4% Outliers: 1.4%

RF: Reflection
$R_{sym} = \Sigma_h\Sigma_i|I_{h,i} - I_h|/\Sigma_h\Sigma_i I_{h,i}$, where I_h is the mean intensity of the i obervations of symmetry related reflections of h. $R = \Sigma|F_{obs} - F_{calc}|/\Sigma F_{obs}$, where $F_{obs} = F_P$, and F_{calc} is the calculated protein structure factor from the atomic model. R.m.s.d. in bond lengths and angles are the deviations from ideal values.

Supplemental Table S1. Summary of crystallography analysis. (related to Figure 1, 4, 7 and Supplemental Figure S6).